

Supporting Information

Gradient adhesion modification of polyacrylamide/alginate-calcium tough hydrogels

Wanglong Zhang, Yiwei Zhang, Yu Dai, Fan Xia, Xiaojin Zhang*

State Key Laboratory of Biogeology and Environmental Geology, Engineering Research Center of Nano-Geomaterials of Ministry of Education, Faculty of Materials Science and Chemistry, China University of Geosciences, Wuhan 430074, China

E-mail: zhangxj@cug.edu.cn

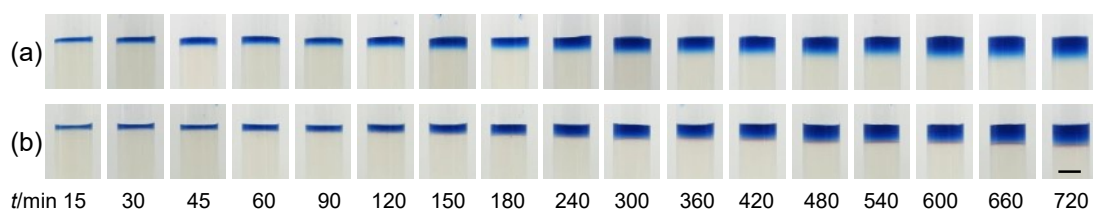


Fig. S1. Images of EDTA diffusion at regular intervals in (a) PAAm/Alg hydrogel and (b) PAAm/Alg- Ca^{2+} hydrogel. Scale bar: 1 cm.

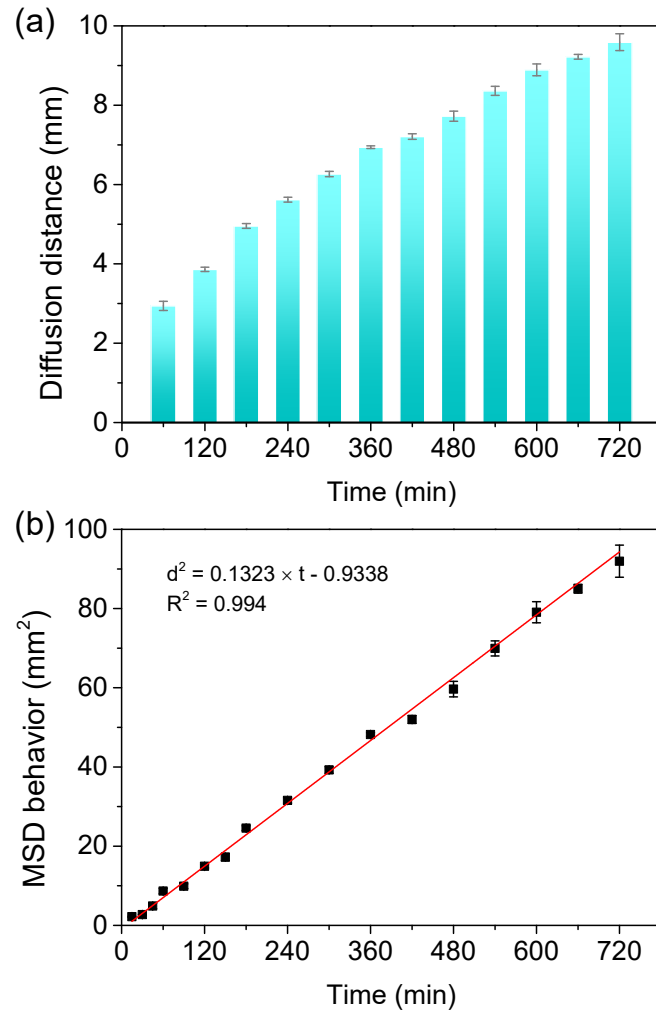


Fig. S2. (a) Diffusion distance of EDTA in PAAm/Alg-Ca²⁺ hydrogel with diffusion time. (b) MSD behavior with diffusion time.

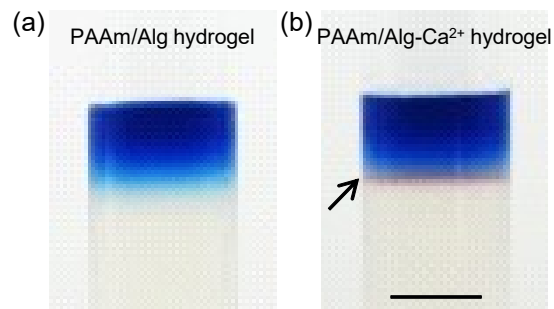


Fig. S3. Enlarged images of EDTA diffusion for 12 h in (d) PAAm/Alg hydrogel and (e) PAAm/Alg-Ca²⁺ hydrogel. The arrow points to a red line. Scale bar: 1 cm.

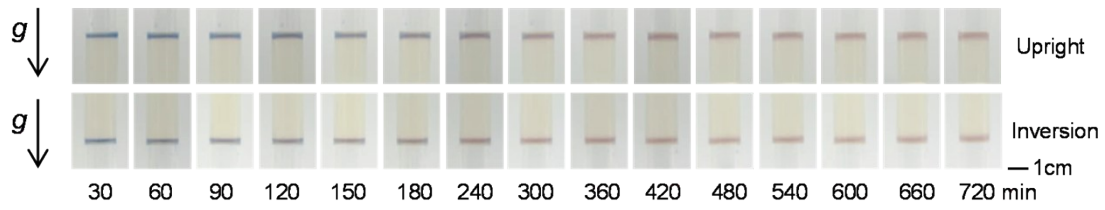


Fig. S4. After 5 min of EDTA diffusion, images of the hydrogel in the upright and inverted state at fixed intervals.

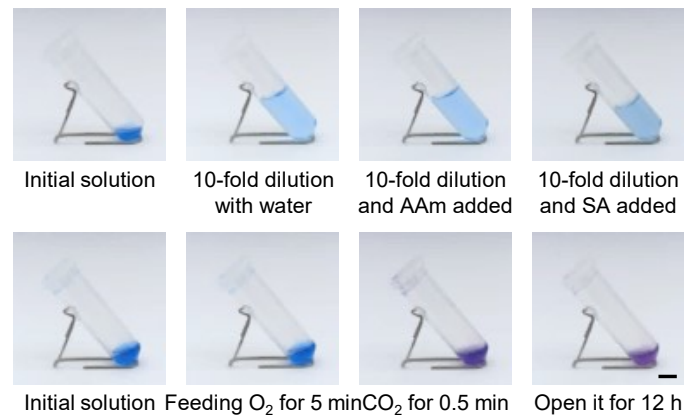


Fig. S5. Images of some solutions to explore the factors affecting red line broadening in PAAm/Alg-Ca²⁺ hydrogel. Scale bar: 1 cm.

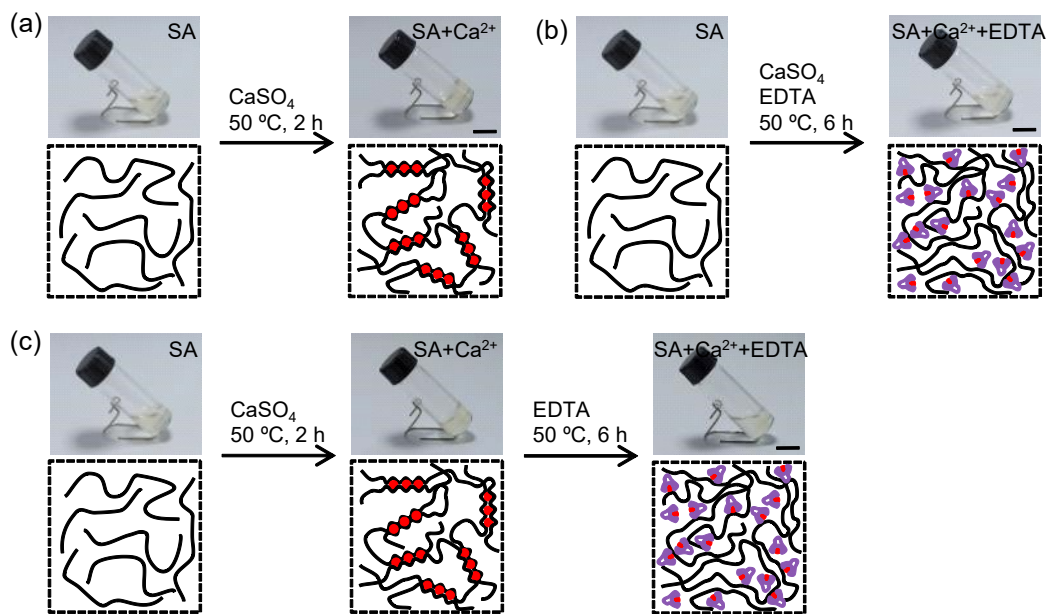


Fig. S6. (a) Image and schematic illustration of the hydrogel formed by SA and Ca²⁺. (b) Image and schematic illustration of the solution formed by SA, Ca²⁺, and EDTA.

(c) Image and schematic illustration of gel-sol transition formed by SA, Ca^{2+} , and EDTA.

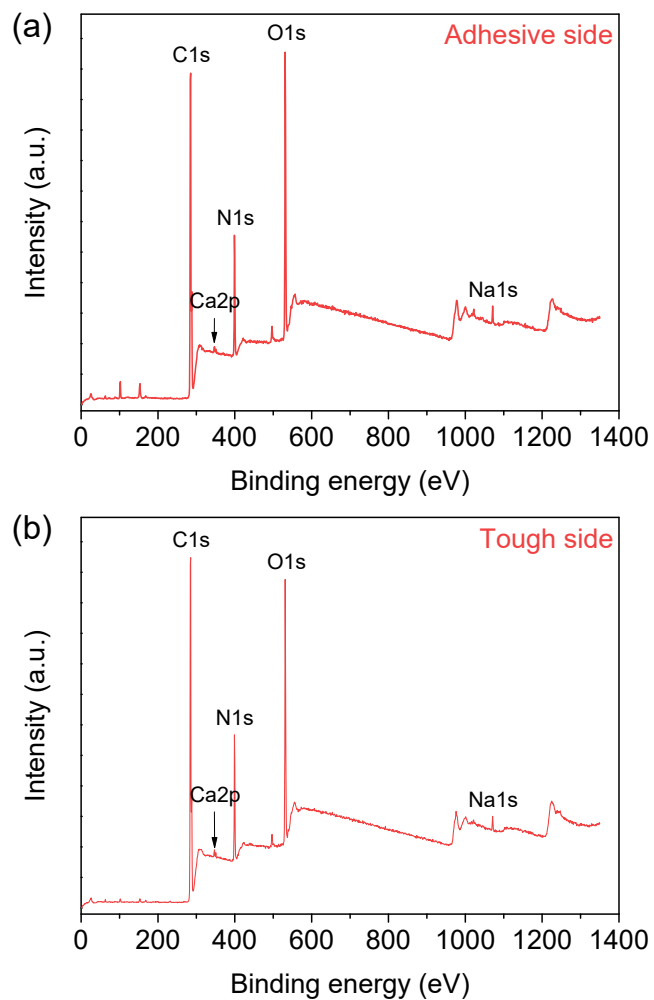


Fig. S7. XPS wide-scan spectra of (a) adhesive side and (b) tough side.

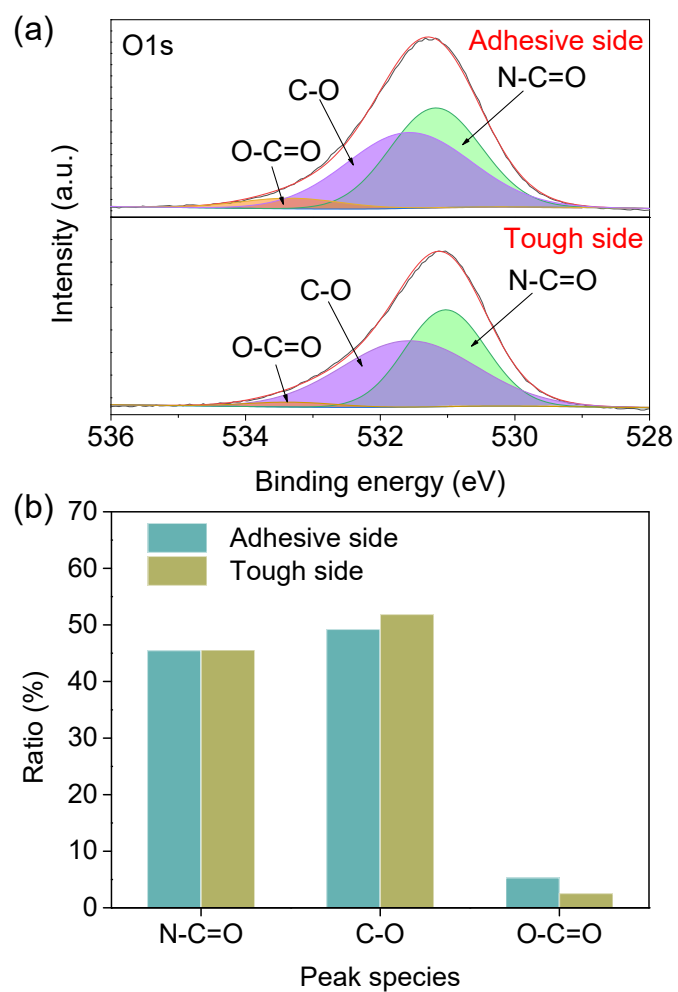


Fig. S8. (a) O1s core-level spectrum and (b) the corresponding peak species ratio of adhesive side and tough side.

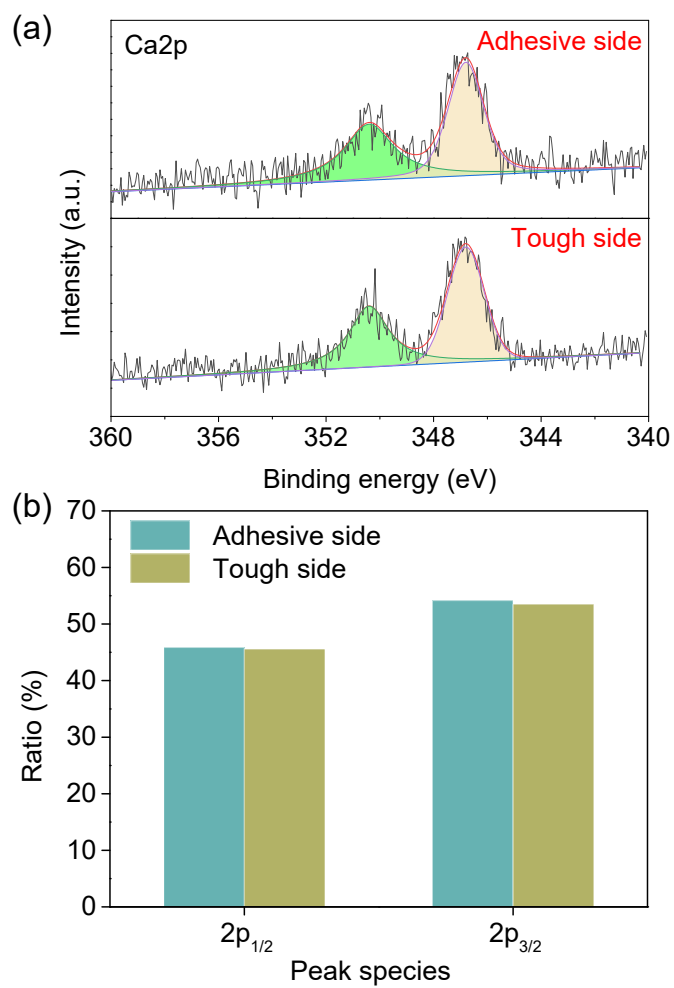


Fig. S9. (a) Ca2p core-level spectra and (b) the corresponding peak species ratio of adhesive side and tough side.

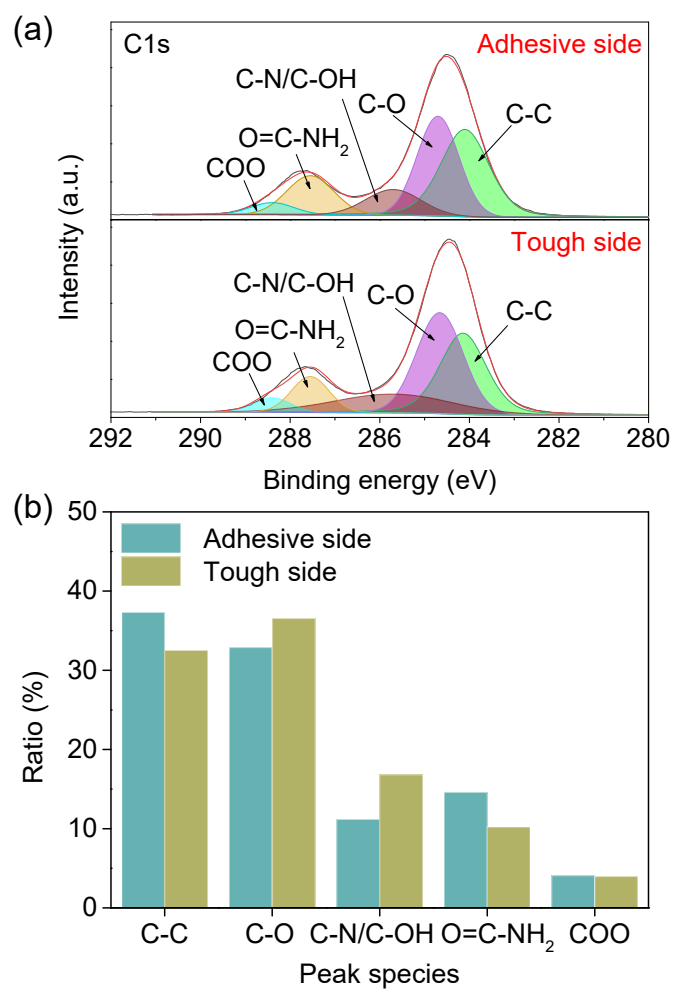


Fig. S10. (a) C1s core-level spectra and (b) the corresponding peak species ratio of adhesive side and tough side.

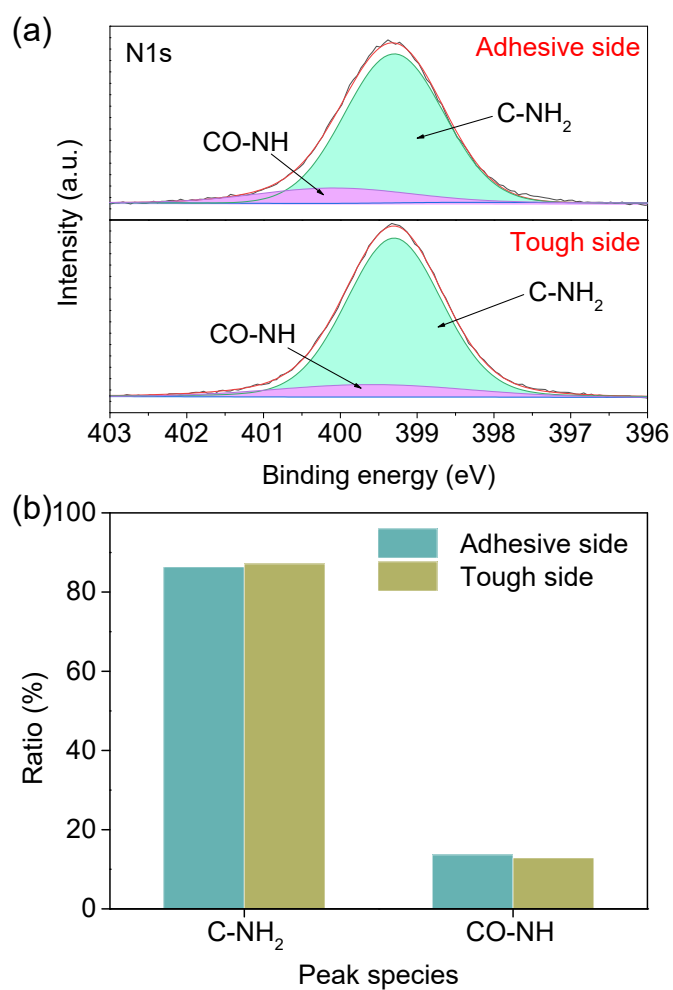


Fig. S11. (a) N1s core-level spectra and (b) the corresponding peak species ratio of adhesive side and tough side.

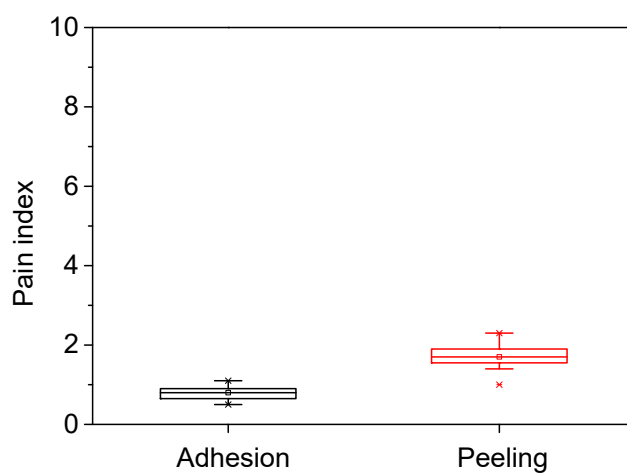


Fig. S12. Pain test on adhesion and peeling process of gradient adhesive-tough hydrogel onto skin (20 volunteers).

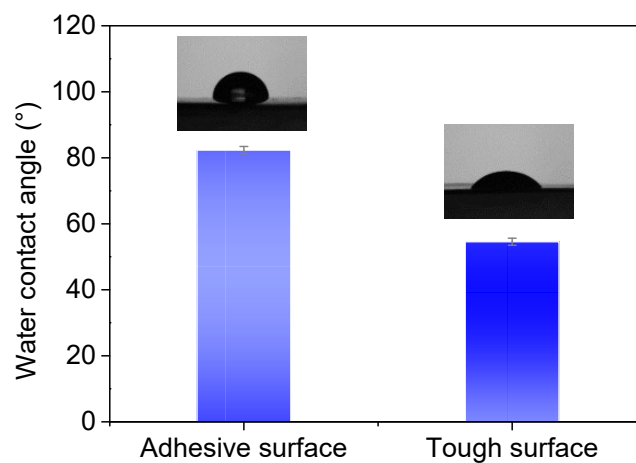


Fig. S13. Water contact angle of adhesive surface and tough surface. $n = 4$ per group. Data are mean \pm s.d.

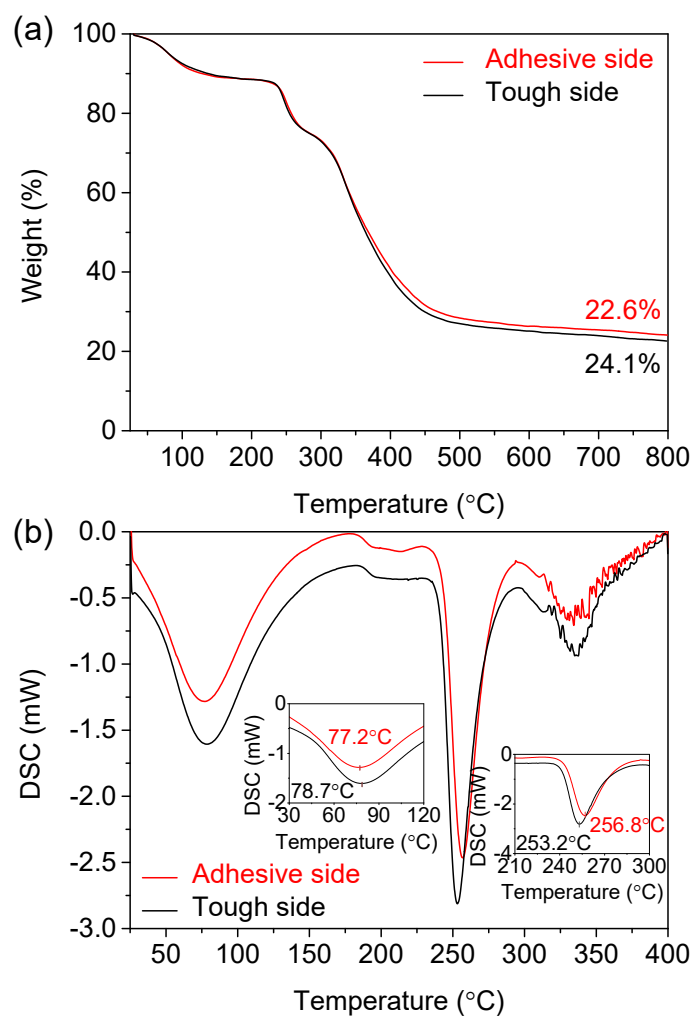


Fig. S14. (a) TG curve and (b) DSC curve of adhesive side and tough side.

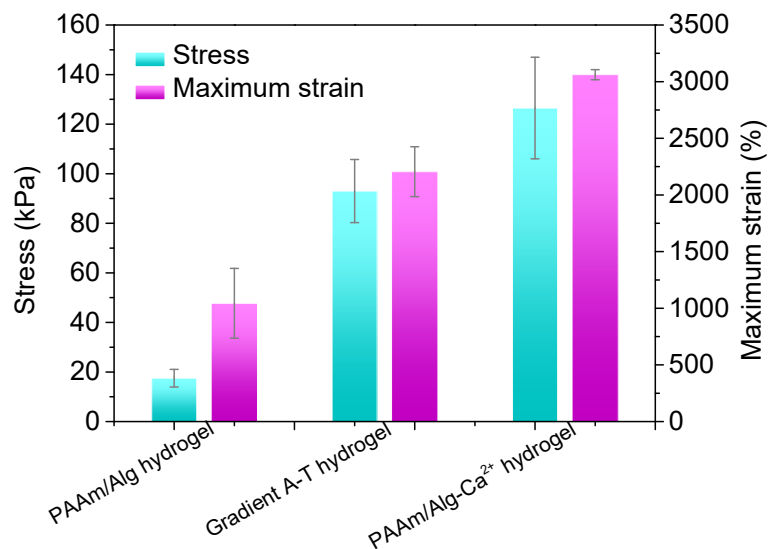


Fig. S15. Stress and maximum strain of hydrogels.

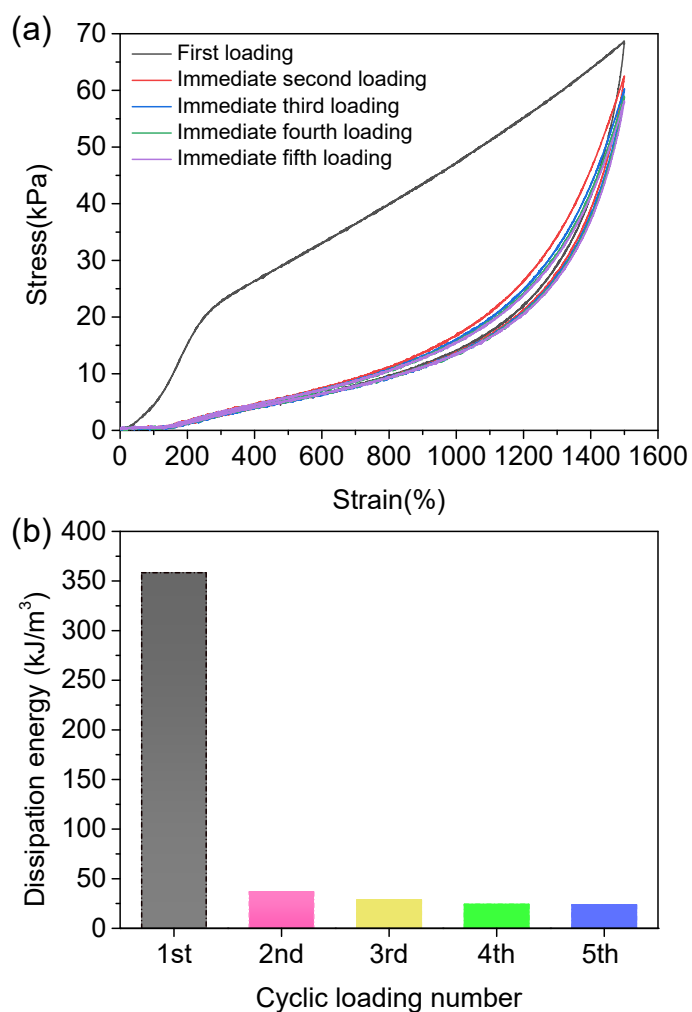


Fig. S16. (a) Successive loading-unloading curves and (b) the corresponding dissipation energy of gradient adhesive-tough hydrogel with no resting time.

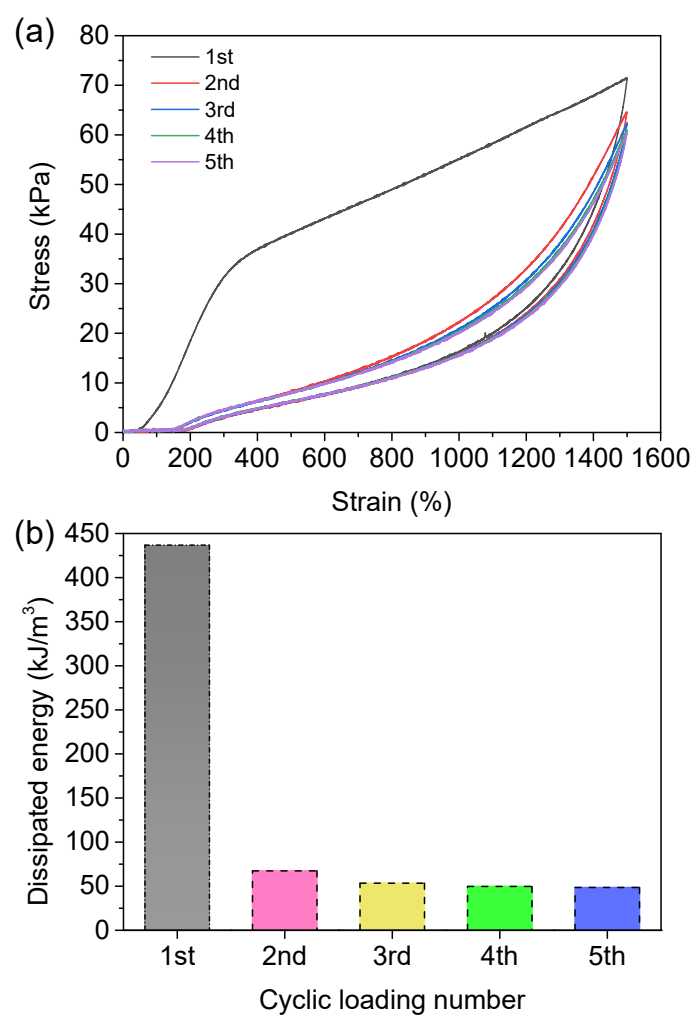


Fig. S17. (a) Loading-unloading curves and (b) the corresponding dissipation energy of gradient adhesive-tough hydrogel with 10 min recovery.

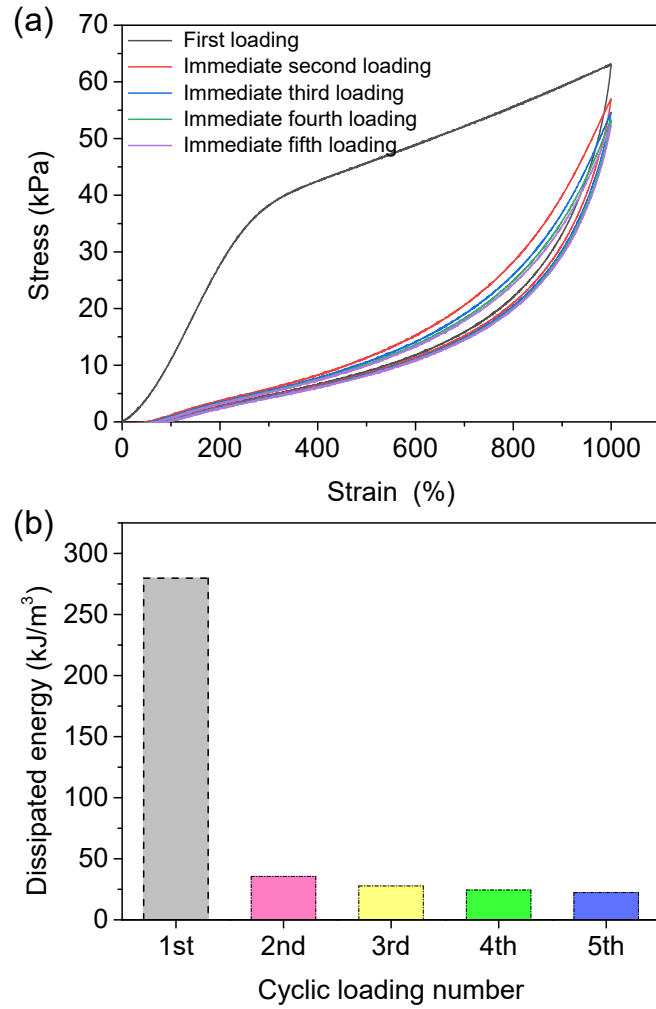


Fig. S18. (a) Successive loading-unloading curves and (b) the corresponding dissipation energy of PAAm/Alg-Ca²⁺ hydrogel with no resting time.

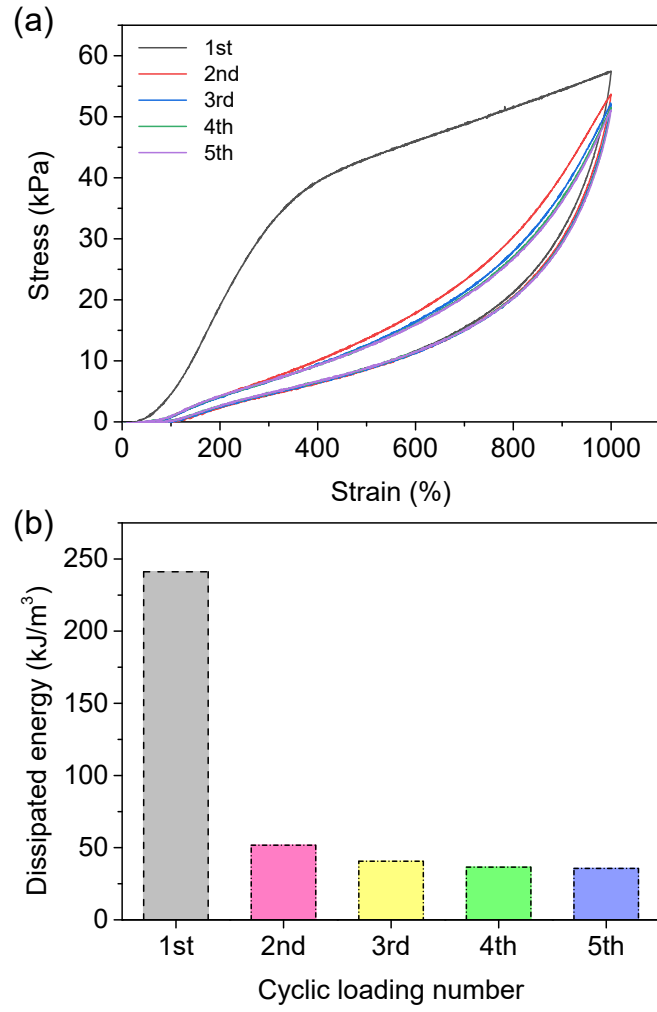


Fig. S19. (a) Loading–unloading curves and (b) the corresponding dissipation energy of PAAm/Alg- Ca^{2+} hydrogel with 10 min recovery.

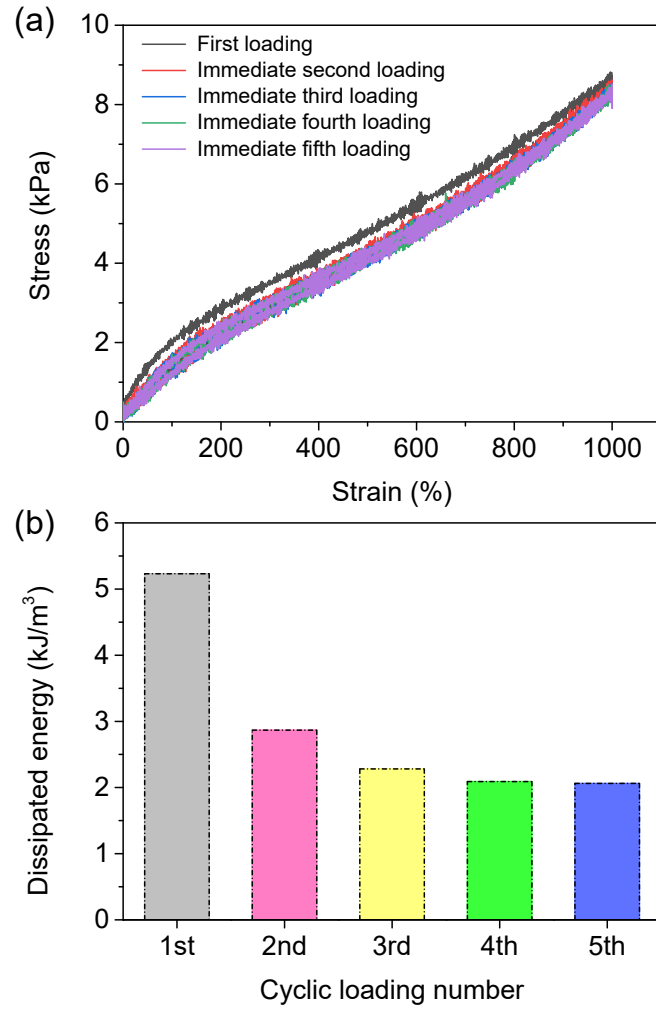


Fig. S20. (a) Successive loading-unloading curves and (b) the corresponding dissipation energy of PAAm/Alg hydrogel with no resting time.

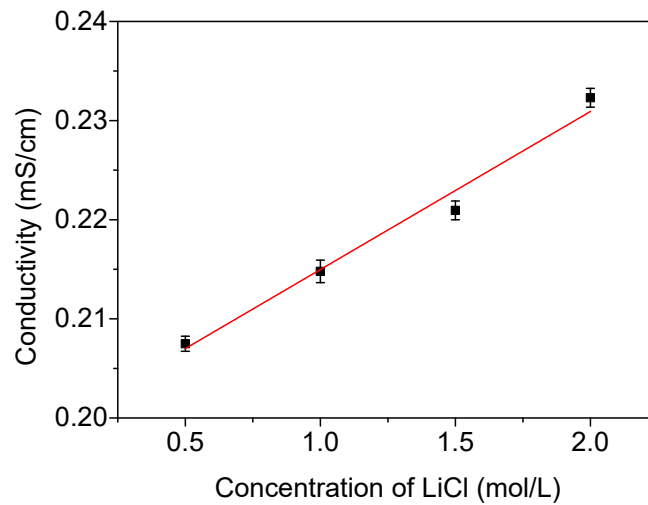


Fig. S21. The conductivity of gradient adhesive-tough hydrogel as a positive

proportional function of the concentration of LiCl.

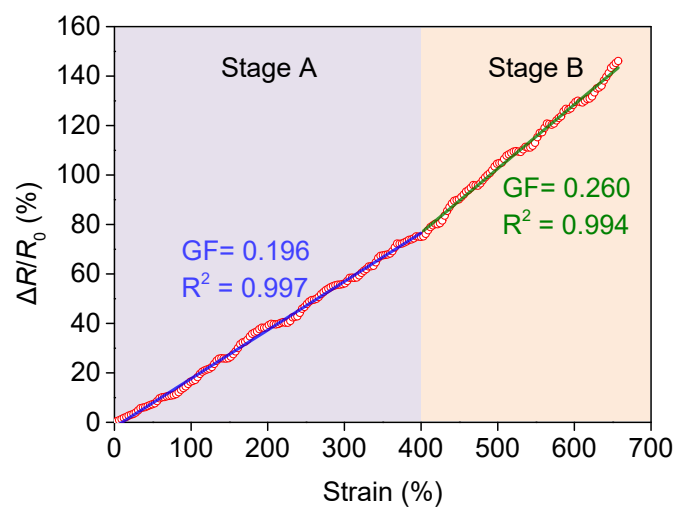


Fig. S22. The relative resistance change of the hydrogel sensor as a function of the applied strain. The gauge factor (GF) can be determined from the slope of the fitted curve.